Iraqi Journal of Veterinary Sciences

www.vetmedmosul.com

Costus-loaded silver nanoparticles mitigated AMPK and related pathways in the albino rat atherosclerosis model

E.A. Jabori[1], H.K. Ismail[2], L.W. Khaleel[1] and A.N. Fliah[2]

[1]Department of Physiology and Biochemistry, College of Veterinary Medicine, University of Baghdad, Bagdad, [2]Department of Pathology and Poultry Diseases, College of Veterinary Medicine, University of Mosul, Mosul, Iraq

Article information

Article history:
Received 17 May, 2023
Accepted 30 July, 2023
Available online 15 December, 2023

Keywords:
Atherosclerosis
Lipid profile
Nanoparticles
Sassurea costus

Correspondence:
E.A. Jabori
dr.anaamanad83@gmail.com

Abstract

In the present study, the role of silver nanoparticles (AgNP)-loaded S. costus was investigated in an atherosclerosis Albino rat model by testing AMP-activated protein kinase (AMPK) genetic pathways and related biomarkers, including apolipoprotein A1 (ApoA1), serum amyloid A (SAA), oxidized low-density lipoprotein (ox-LDL), visfatin, and lactate dehydrogenase enzyme (LDH). This pathway has been identified as a key regulator of cellular metabolism and energy homeostasis. Also, it is linked to atherosclerosis, a chronic inflammatory disease that affects arterial walls and is a major cause of cardiovascular disease. Nanoparticles in medicine have gained attention due to their unique properties and potential applications. One such nanoparticle that has shown promising results in treating atherosclerosis is silver nanoparticles. The costus extract was prepared and characterized to do so, followed by the synthesis of costus-loaded nanoparticles. The synthesized product was characterized by various methods, including UV-visible spectrometry, Fourier transform infrared, X-Ray diffraction, scanning electron microscope, Atomic Force Microscopy, and Energy dispersive spectroscopy. Rats were treated with costus-loaded nanoparticles. The results of AMPK gene pathways and related biomarkers (ApoA1, SAA, oxLDL, visfatin, and LDH) were measured and compared between positive and negative control groups. The results have confirmed that costus-loaded nanoparticles have greatly influenced and reduced AMPK gene pathways and related biomarkers (ApoA1, SAA, ox-LDL, visfatin, and LDH) compared to the positive control group of atherosclerosis rat models. The study concluded that costus-loaded nanoparticles are important in atherosclerosis and improve rat status by reducing the genetic and proteomic pathways linked to atherosclerosis.

DOI: 10.33899/ijvs.2023.140352.3039, ©Authors, 2024, College of Veterinary Medicine, University of Mosul.

Introduction

The AMP-activated protein kinase (AMPK) pathway is a highly conserved signaling pathway crucial in maintaining cellular energy homeostasis in eukaryotic cells. This pathway is activated in response to decreased cellular energy levels, such as during exercise, fasting, or glucose deprivation. Once activated, AMPK promotes the production of ATP, the primary energy source for cells, while inhibiting energy-consuming processes, such as protein and fatty acid synthesis. Thus, AMPK is a central regulator of cellular energy metabolism, ensuring that cells have enough energy to perform their necessary functions (1,2). Atherosclerosis is a chronic and complex inflammatory disease affecting the arteries and is considered one of the leading causes of cardiovascular diseases. This disease is characterized by the accumulation of lipids, immune cells, and other substances in the inner lining of the arteries, which leads to the formation of plaques. These plaques cause the arteries to narrow and restrict blood flow, leading to serious consequences such as heart attacks, strokes, and other cardiovascular complications (3). AMPK activation has been shown to have anti-atherogenic effects through several mechanisms, including inhibiting lipid synthesis and promoting cholesterol efflux from macrophages (4). Additionally, AMPK activation can suppress the production of pro-inflammatory cytokines and chemokines by immune cells, thereby reducing the recruitment of inflammatory cells to the arterial wall (2,5). Moreover, AMPK activation can enhance endothelial cell function and promote angiogenesis, which can help to restore blood flow to ischemic tissues (6). Several plant products are modulating AMPK activators (7-9) and have been shown to have beneficial effects on atherosclerosis in preclinical and clinical studies. However, the precise mechanisms underlying these effects are still not fully understood, and further research is needed to elucidate the role of AMPK signaling in atherosclerosis and to develop new therapeutic strategies targeting this pathway. In summary, the AMPK pathway is a promising target for the prevention and treatment of atherosclerosis, and further studies are needed to fully exploit its potential benefit in this disease (10). Researchers conducted studies to identify the therapeutic roles of nanoparticles in different diseases status (11-14).

Therefore, in the present study, we explored the role of silver nanoparticles on the modulation of atherosclerosis in certain aspects using a well-known antiatherosclerotic costus plant as a loading plant.

Materials and methods

Ethical approve

The scientific committee has approved this study of the college of veterinary medicine- University of Baghdad at the seventh congress dated 11/1/2022, that the concurrent conducting experiment did not violent the laws of animal rights and the euthanasia is applied in accordance of this guidelines, and approval issue number and date is UM.VET.2022.014.

Costus extract and nanoparticle formulation

The utilization of plants to create silver nanoparticles is more advantageous than using other biological processes, and every year, more publications (about 468 in 2020) report using plant extracts in the production of nanoparticles were reported. Green-produced nanoparticles with antioxidant and cytotoxic capabilities may be viable for advancing nanomaterials due to the economic benefits of employing plants in biosynthesis and the lack of need for hazardous chemicals or processes. In the present study, Costus has been used due to its common therapeutic potential.

Effective dose determination

The effective dose after 14 days of treatment with *Sassurea costus* loaded AgNPs (Figure 1).

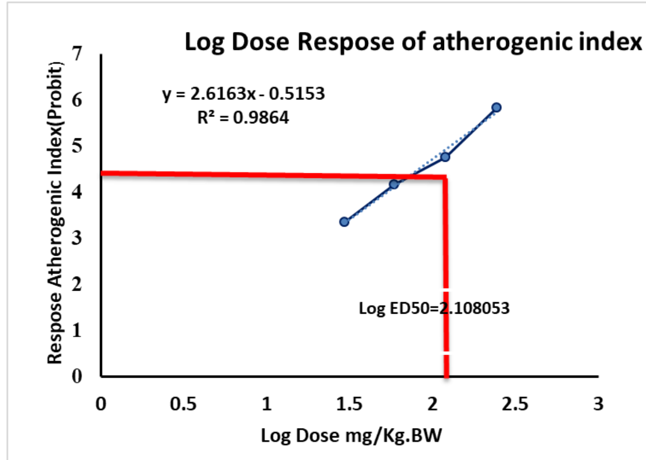

Figure 1: Reveals the effect of successive doses of AgMSNPs on the atherogenic index after 14 days in adult rats.

The experimental animal models

36 male Albino rats age 4 weeks; weight 200-250g were for this experimental trial. The rats were kindly provided by the animal house/College of Veterinary Medicine/University of Mosul and were fed a standard commercial meal and housed at a stable temperature of 22-25ºC. Before the trial, the rats were acclimated for 7 days and split into four groups, each consisting of five rats. Group 1: The control group was treated with distal water orally for 12 days. Group 2: Control positive treated with H_2O_2 (1%) +cholesterol. Group 3: Control positive treated with H_2O_2 (1%)+cholesterol+costus. Group 4: Control positive treated with H_2O_2 (1%) +cholesterol+ costus loaded silver nanoparticles.

Blood sampling

Blood samples were taken from rats after 14 days of experimentation. A capillary tube was implanted in the inner corner of the eyeball to draw blood from the eye vein. The blood was placed in gel tubes, clotted, and separated using a centrifuge. The serum was stored in the refrigerator for further analysis. Ethylene diamine tetra acetic acid (EDTA) was used to take blood samples for manual hematological analysis. The Leishman stain was used for blood smear staining to analyze physiological parameters. The serum was used for biochemical analysis, including ApoA1, oxLDL, SAA, Visfatin, and LDH measurement.

Preparation of Silver Nanoparticle: a 1 mM AgNO3 solution was prepared by dissolving 4.56 gms of silver nitrate in 200 ml of deionized distilled water. The solution was mixed with an ultrasonic water bath for 20 minutes and placed in a dark place to avoid auto-oxidation. The study involved modifying a method for preparing silver nanoparticles using vitamin C as a reducing and capping agent. The mixture is left for an hour and monitored for a color change indicating the formation of silver nanoparticles.

The residue is washed and dried before being stored in dark bottles at 4 ˚C. Different methods characterize AgNPs, including UV-visible spectrometry, FT-IR, XRD, SEM, AFM, and EDS.

Collection of plant

In February 2021, roots of *Sassurea costs* were collected from an Indian province and were identified and verified by a taxonomist in Baghdad's Directorate of Seed Testing and Certification. The plant was classified as a Saussurea species and belongs to the Asteraceae family.

Extraction of plant

The process of extracting plant material using methanol as a solvent. The ground plant material was air-dried and extracted using the Soxhlet method with 80% v/v methanol: water for 8 hours. The resulting extracts were concentrated, dried, and stored in a refrigerator until further use (15).

Characterization of AgNPs

Various methods assessed the biosynthesized silver nanoparticles, including visual color changes, UV-visible spectrometry, FT-IR, XRD, SEM, AFM, and EDS. The UV-visible spectroscopy method is important for evaluating and determining the synthesized AgNPs in an alcohol solution. The Shimadzu UV-1600 in the Ministry of Science and Technology labs was used for this purpose. A brown color shift in the reaction was observed due to the Plasmon resonance peak for the silver nanoparticles. The peak was located between 450 and 550 nm. The strong band in the spectral pattern is caused by the stimulation of localized surface plasmons, which causes intense light scattering by an electric field at a wavelength where resonance occurs.

The text explains using X-Ray Diffraction (XRD) to analyze phase identification and crystallization of nanoparticles, particularly *Sassurea costus* AgNPs particles. XRD provides information on particles' metallic nature, size, shape, and electron density. It works by diffracting light at various angles when an X-ray passes through a crystal, creating a diffraction pattern that reveals the atomic arrangement inside the crystal. The silver nanoparticles were analyzed using XRD in the Ministry of Research and Technology labs with a 6000/Shimadzu instrument from Japan.

The scanning electron microscope (SEM) records secondary electrons emitted from the sample by the electron beam impinging on it, providing three-dimensional morphology of objects. The electron beam is concentrated to small points by magnetic lenses and driven back and forth over the object by scanning coils. This examination was done at the Ministry of Science and Technology labs using Tescan Vega I/Czech SEM to analyze the morphology of samples. To analyze *Sassurea costus* AgNPs, a drop is placed on a clean slide, and the water is allowed to fully evaporate.

The article describes using an atomic force microscope (AFM) to examine the topography of a material. The AFM uses a nano-sized tip connected to a cantilever to generate a 3D picture of the sample topography. The AFM is preferred over the SEM for detecting and examining the size and shape of silver nanoparticles in three dimensions and is used to determine their height.

EDS (Energy Dispersive Spectroscopy) was used to determine the elemental composition of a reaction mixture using the INCA Energy 250 system from Oxford, Japan.

Effective dose determination

The experiment aimed to determine the effective dosage of *Sassurea costus* AgNPs on various parameters in adult male rats. 30 rats were randomly assigned to six groups, with one group as a control, and the others were given different doses of *Sassurea costus* AgNPs orally for 14 days. The rats were monitored for toxicity and death, and blood samples were analyzed before euthanizing. The analysis included lipid profile, hematological analysis, atherogenic index, and biochemical and physiological parameters using Leishman stain on blood smear staining.

Genetic analysis

The text uses two primers, one for the B-actinin gene and another for the AMPK gene (Table 1), to measure gene expression through qRT-PCR methods. The primers were created using data from NCBI-Gene Bank and Primer 3 online and were assisted by Bioneer in using Ethidium bromide DNA binding dye.

Table 1: Forward and reverse of designed primers

Primers	Sequence	Primer sequence	Tm(°C)	GC (%)
AMPK	F	GACCTGAAGCCAGAGAACGTG	63.3	57
	R	AGCCTTCCTGAGATGACCTCC	64.8	57
B actin	F	GAGGGAAATCGTGCGTGACAT	62.2	52
	R	AACCGCTCATTGCCGATAGTG	61.5	52

The Synthesis SuperMix for qPCR is an incredibly useful kit for researchers looking to synthesize cDNA from total RNA or mRNA. The kit contains all the necessary components, allowing researchers to perform simultaneous genomic DNA removal and cDNA synthesis. The resulting cDNA is suitable for qPCR but not for regular PCR. This is because standard PCR requires longer DNA fragments than qPCR, which targets smaller fragments. The kit is provided at a concentration of 5× and is used at a concentration of 1× by adding gDNA remover, RNA, and H_2O. This makes it incredibly easy to use, as researchers don't need to worry about measuring out different components or worrying about what they might be missing. The kit also includes a gDNA remover, which helps to remove any genomic DNA that might be present in the sample. This is important because genomic DNA can interfere with qPCR results, leading to inaccurate readings. After the cDNA synthesis, the gDNA remover and reverse transcriptase are inactivated by heating at 85ºC for 5 seconds. This step is crucial in ensuring that the cDNA is suitable for qPCR and that any remaining reverse transcriptase or gDNA remover won't interfere with the qPCR results. Overall, the Synthesis SuperMix for qPCR is an incredibly useful tool for researchers looking to synthesize cDNA from total RNA or mRNA. It simplifies the process by providing all the necessary components and allows researchers to perform simultaneous genomic DNA removal and cDNA synthesis. The resulting cDNA is suitable for qPCR and is easy to use, making it an essential kit for any researcher working with qPCR.

The EasyScript First-Strand cDNA Synthesis SuperMix kit contains all the necessary components for cDNA synthesis from total RNA or mRNA. It includes the EasyScript RT/RI Enzyme Mix and 2×ES Reaction Mix, which efficiently synthesize cDNA. The kit also has deficient Rase H activity to reduce RNA template degradation during the first-strand cDNA synthesis. The product obtained from 15 minutes reaction is used for qPCR, while the product obtained from 30 minutes reaction is used for PCR. The kit includes an Anchored Oligo(dT) Primer that binds to the first base next to mRNA Poly(A)* on the 5' end with high specificity, ensuring high efficiency and success rate of first-strand cDNA synthesis.

The procedure for performing Quantitative RT-PCR using the GoTaq® qPCR Master Mix kit contains primers, cDNA samples, and water. The B actin gene is used as the endogenous control, and the qPCR is conducted at 95°C for 1 minute, followed by 45 cycles of denaturation and annealing. Finally, melting curve analysis is performed based on the characteristics of double-stranded cDNA during cycles. The text describes a method for determining the expression of target genes using the comparative Ct formula and Folding =2^-ΔΔCT analysis. The Ct value of the target genes is standardized to the B actin reference gene. The reaction is mixed, centrifuged, and stored on ice before being placed in a thermal cycler that is programmed accordingly.

Measurement of visfatin, ApoA1, oxLDL, and SAA

The ELISA kits for measurement of visfatin, ApoA1, oxLDL, and SAA (Elabscience, USA) use the Sandwich-ELISA principle to detect Rat visfatin, ApoA1, oxLDL, and SAA concentration. A micro-ELISA plate is pre-coated with an antibody specific to Rat visfatin, ApoA1, oxLDL, and SAA. The process for measuring the concentration of Rat VF in samples using a biotinylated detection antibody and Avidin-HRP conjugate. The process involves measuring the OD value spectrophotometrically at 450 nm ± 2 nm and comparing it to a standard curve. Additionally, the text mentions that LDH can detect cell damage or cell death.

Results

Visual observation or color modification of biosynthesized silver nanoparticle (AgNPs)

The initial stage in the fabrication of biogenic AgNPs utilizing alcohol extract to ensure costus is to adjust the particle color (AgNPs). When the *Sassurea costus* extract was added to the colorless silver nitrate solution (Figure 2), the color of the combination changed to brownish after 20 minutes. The color began to alter from white Transparent to dark lead of silver nanoparticles after 48 hours.

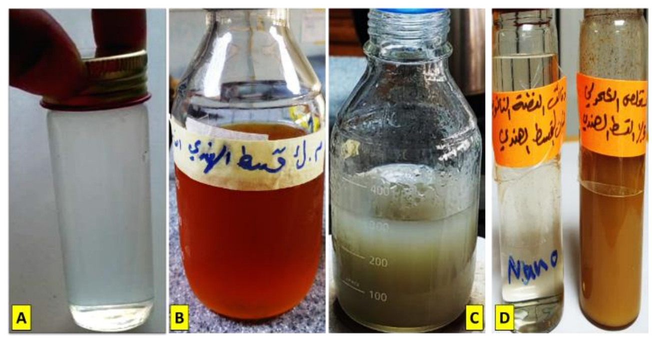

Figure 2: Explain the Color change during the formation of Silver Nanoparticles: A-$AgNO_3$ only. B-Chang in color from brown to silver when put the mint extract drop by drop. C-Chang the color after 2 hours from reaction time. D-Depositions of particles (centrifuge and wash). E-The AgNPs after two days.

UV-Visible spectroscopy Ag nanoparticles

The optical absorbance of manufactured AgNPs was evaluated by (UV-Vis) spectroscopy. The existence of AgNPs is confirmed by an absorbance peak 215 nm (Table 2).

Table 2: UV-VIS peak values of extract of AgNPS, *Sassurea costus*, and AgNPs *Sassurea costus*

No	Wavelength	Abs
AgNPs	215	3.436
AgNPs *Sassurea costus*	224	3.524
Sassurea costus	271	0.509

FT-IR spectrum of alcohol roots extract of AgNPs *Sassurea costus*: FT-IR analysis was carried out to identify major functional groups present at different positions in the root extract of *Sassurea costs*. The obtained peaks in the FT-

IR spectrum of silver were compared for best matches with libraries of spectra cataloged for available material (Figure 3).

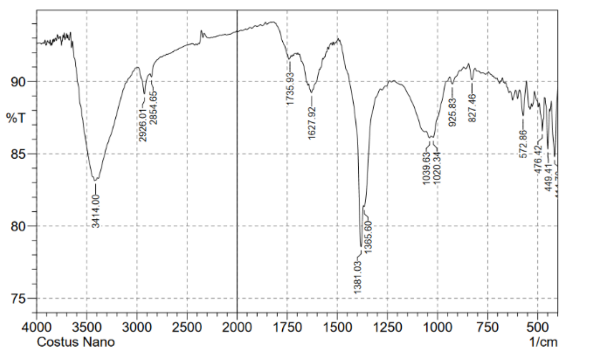

Figure 3: FT-IR spectrum of Biogenic AgNPs.

X-Ray diffraction (XRD)

The XRD pattern is an important tool used in material science to describe the crystalline nature of a substance. In figure 4, the XRD pattern describes the biosynthesized silver nanoparticles (AgNPs), which occur due to metal ions (Ag+) reduction by the bioactive compounds present in a plant extract. This process is of great interest to researchers because it provides a sustainable and green approach to synthesizing silver nanoparticles, widely used in various fields such as medicine, electronics, and environmental science. The XRD pattern shows the diffraction peaks of the AgNPs, which are characteristic of their crystalline structure. The equation used to describe the process of biosynthesis provides a quantitative understanding of the process and helps researchers to optimize the conditions for the synthesis of AgNPs. The biosynthesis of AgNPs using plant extracts is a promising area of research that has the potential to replace conventional methods that use toxic chemicals. The XRD pattern and the equation used to describe the process provide valuable information that can be used to improve the synthesis of AgNPs and make them more sustainable and environmentally friendly.

Scanning electron microscopy (SEM) analysis for AgNPs

The image SEM, or Scanning Electron Microscope, is a powerful tool that allows us to see the intricate details of the biosynthesized silver nanoparticles using *S. costus* root extracts. Figure 5 reveals that the nanoparticles are small and highly aggregated, with some larger nanoparticles associated with a spherical shape. This suggests that the aggregation process may have influenced the final shape of the nanoparticles. In addition, the image shows that some particles were scattered. In contrast, others were mixed, indicating that the time after synthesis may have played a role in the final distribution of the nanoparticles. Overall, the SEM image provides valuable insight into the structure and characteristics of the biosynthesized silver nanoparticles, which can help researchers better understand their properties and potential applications. By utilizing advanced imaging techniques like SEM, we can continue to push the boundaries of scientific discovery and innovation.

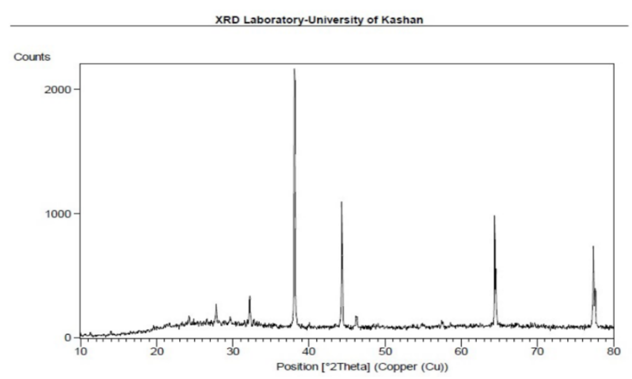

Figure 4: The XRD pattern of biosynthesized AgNPs

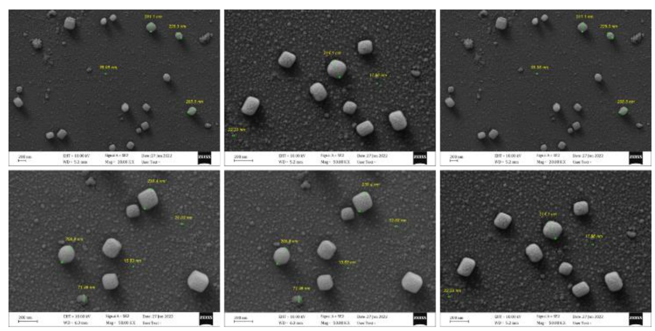

Figure 5: Scanning Electron Microscope image for Biogenic AgNPs.

Atomic force microscopy (AFM) of *Sassurea costus* AgNPs

The size and colloidal stability of nanoparticles are crucial factors that determine their properties and applications. In this context, the extract used in the synthesis of nanoparticles plays a big role. The extract helps control nanoparticle size, shape, and stability. The study found that alcohol AgNPs had a thin, flat shape with a thickness between 0.5 and 2.7 nm (Figure 6). This finding is significant because it indicates that the extract used in the synthesis of alcohol AgNPs has a strong influence on their morphology and physical properties. The AFM analysis of the surface topography further confirmed the thin and flat shape of alcohol AgNPs. This information is useful for researchers and engineers interested in developing new nanoparticle applications. By understanding the extract's role in controlling the size and shape of nanoparticles, researchers can design more efficient and effective methods for synthesizing nanoparticles with specific properties and characteristics. Overall, the study provides valuable insights into the synthesis and characterization of nanoparticles, which can help advance the nanotechnology field.

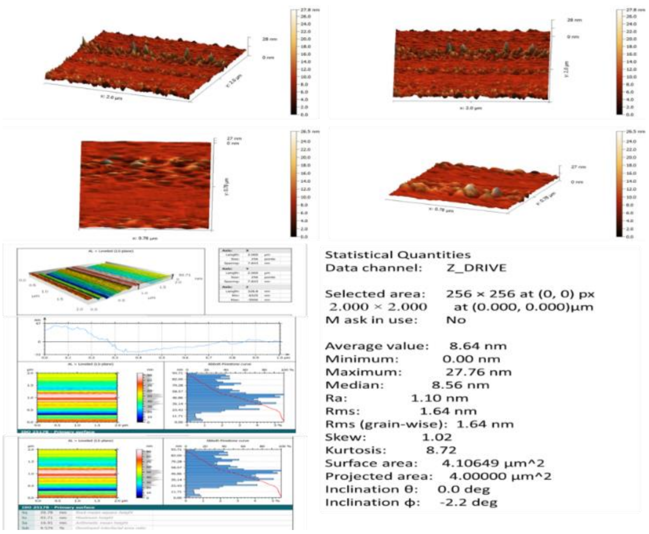

Figure 6: Atomic force microscopy (AFM) for silver nanoparticles was synthesized by alcohol extract of *S. costus*. (AgNPs) Two-dimensional image (a), three-dimensional image (b), Size Range of Biogenic Silver Nanoparticles (c), and (d).

Energy dispersive spectroscopy (EDS) analysis of Sassurea costus AgNPs

Energy dispersive spectroscopy (EDX) of the spectrum reveals a strong signal in the silver region and confirms the formation of AgNPs (Figure 7).

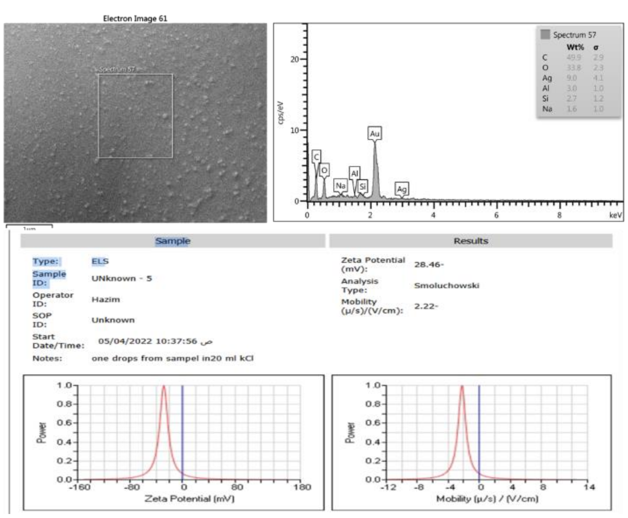

Figure 7: Energy dispersive spectroscopy (EDS) analysis of *Sassurea costus* AgNPs.

Induction of atherosclerosis

The induction of atherosclerosis (G2, G3, and G4) has shown a statistically significant increase in plasma concentrations of ApoA1 compared to the negative control group. However, ApoA1 was elevated alongside using the diet with cholesterol alone (G3) and cholesterol+ H_2O_2 (G4), compared to the H_2O_2 alone (G2) group. Moreover, a combination of cholesterol+ H_2O_2 (G4) has significantly elevated ApoA1 than using either alone. The induction of atherosclerosis (G2, G3, and G4) has demonstrated a significant elevation of plasma concentrations of oxLDL compared to the negative control group. However, oxLDL was elevated alongside using the diet with cholesterol alone (G3) and cholesterol+ H_2O_2 (G4), compared to the H_2O_2 alone (G2) group. Moreover, a combination of cholesterol+ H_2O_2 (G4) has significantly elevated oxLDL than using either alone. The induction of atherosclerosis (G2, G3, and G4) has shown significantly higher plasma concentrations of SAA compared to the control group. However, SAA was elevated alongside using the diet with cholesterol alone (G3) and cholesterol+ H_2O_2 (G4), compared to the H_2O_2 alone (G2) group. The induction of atherosclerosis (G2, G3, and G4) has shown a significant increase in plasma concentrations of visfatin compared to the control group. However, visfatin was elevated alongside using the diet with cholesterol alone (G3) and cholesterol+ H_2O_2 (G4), compared to the H_2O_2 alone (G2) group. Moreover, a combination of cholesterol+ H_2O_2 (G4) has significantly elevated visfatin than using either alone. The induction of atherosclerosis (G2, G3, and G4) has shown significantly higher plasma LDH concentrations than the control group. However, LDH was elevated alongside using the diet with cholesterol alone (G3) and cholesterol+ H_2O_2 (G4), compared to the H_2O_2 alone (G2) group. Moreover, a combination of cholesterol+ H_2O_2 (G4) has significantly elevated LDH than using either alone (Figure 8).

Nanoparticle treatment of atherosclerotic model

The ApoA1 has significantly elevated in the H_2O_2+cholesterol (G2) group, costus-treated group (G3), and costus-loaded nanoparticles (G4) compared to G1 (control) group. H_2O_2+cholesterol (G2) group has a significantly higher ApoA1 compared to the control group, costus-treated group (G3), and costus-loaded nanoparticles (G4). Weak differences existed between ApoA1 levels of the costus-treated group (G3) and costus-loaded nanoparticles (G4). The SAA has significantly elevated in the H_2O_2+cholesterol (G2) group, costus-treated group (G3), and costus-loaded nanoparticles (G4) compared to G1 (control) group. H_2O_2+cholesterol (G2) group has a significantly higher SAA compared to the control group, costus-treated group (G3), and costus-loaded nanoparticles (G4). No differences existed between SAA levels of the costus-treated group (G3) and costus-loaded nanoparticles (G4). The ox-LDL has significantly elevated in the

H_2O_2+cholesterol (G2) group, costus-treated group (G3), and costus-loaded nanoparticles (G4) compared to G1 (control) group. H_2O_2+cholesterol (G2) group has a significantly higher oxLDL compared to the control group, costus-treated group (G3), and costus-loaded nanoparticles (G4). Weak differences existed between oxLDL levels of the costus-treated group (G3) and costus-loaded nanoparticles (G4). The visfatin has significantly elevated in the H_2O_2+cholesterol (G2) group compared to G1 (control) group. Costus-treated group (G3) and costus-loaded nanoparticles (G4) have significantly reduced LDH compared to H_2O_2+cholesterol (G2) group. No differences existed between visfatin levels of the costus-treated group (G3), costus-loaded nanoparticles (G4), and control group. The LDH has significantly elevated in the H_2O_2+cholesterol (G2) group compared to G1 (control) group. Costus-treated group (G3) and costus-loaded nanoparticles (G4) have significantly reduced LDH compared to H_2O_2+cholesterol (G2) group. No differences existed between LDH levels of the costus-treated group (G3), costus-loaded nanoparticles (G4), and control group (Figure 9).

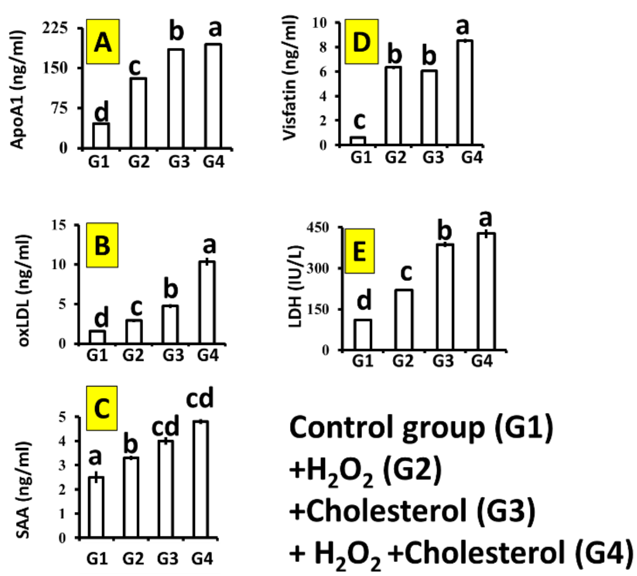

Figure 8: Blood biomarkers in atherosclerosis induced model of the studied group. Data expressed as mean±SD, abcd $p<0.05$. ApoA1=apolipoprotein, oxLDL=oxidized low-density lipoprotein, SAA=Serum amyloid A, LDH=lactate dehydrogenase enzyme.

Gene expression profile and subsequent suppression by costus-loaded nanoparticles

The AMPK gene expression has been calculated as a fold of changes concerning the housekeeping gene; the outcome revealed that AMPK gene expression is higher in the cholesterol+ H_2O_2 (G2) group compared to the control (G2) group, costus-treated group (G3), and costus-loaded nanoparticles (G4). The study has confirmed that the costus-treated group (G3) and costus-loaded nanoparticles (G4) have significantly reduced AMPK gene expression (Table 3).

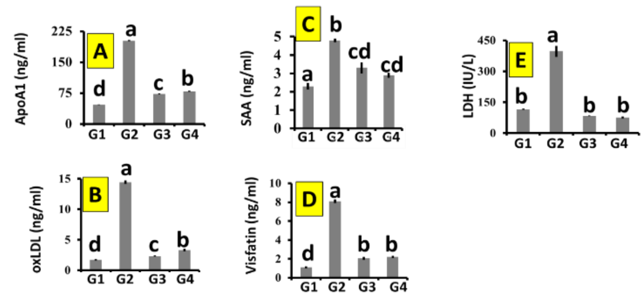

Figure 9: Silver nanoparticles have improved the measured parameters linked to atherosclerotic diseases. ApoA1=apolipoprotein, oxLDL=oxidized low-density lipoprotein, SAA=Serum amyloid A, LDH=lactate dehydrogenase, G1=Control, G2= H_2O_2+cholesterol, G3=extract plant, G4=plant loaded with nanoparticles.

Table 3: AMPK gene expression induced by costus-loaded nanoparticles compared to costus alone, positive, and negative groups fold of changes relative to a housekeeping gene.

Group	AMPK gene
Control	1.617 ± 0.496 B
H_2O_2+cholesterol	2.265 ± 0.443 A
Extract plant	1.390 ± 0.148 C
Plant loaded with nanoparticles	1.120 ± 0.526 D

Discussion

Nanoparticles have become increasingly popular in various fields, including medicine, energy, and electronics. However, recent research has shown that their impact on human health is still largely unknown. One area of concern is the potential impact of nanoparticles on cardiovascular health (16). Studies have found that nanoparticles can reduce the production of Apolipoprotein A, which plays a critical role in maintaining healthy cholesterol levels (17). This reduction in production could lead to a buildup of cholesterol in the bloodstream, which increases the risk of heart disease. One possible explanation for the effect of nanoparticles on Apolipoprotein A is that they interfere with the liver's normal function (18). The liver produces Apolipoprotein A, and nanoparticles may disrupt this process, leading to decreased production. Another possibility is that nanoparticles could bind to Apolipoprotein A, preventing it from performing normal bodily functions (19). The impact of nanoparticles on human health is still largely unknown, and while some studies have suggested negative health effects, others have found no significant impact (20). This uncertainty highlights the need for caution when considering the use of nanoparticles in various applications. It is important to carefully consider nanoparticles' potential risks and benefits, particularly regarding human health. As researchers continue to study the potential impact of nanoparticles on human health, the goal should be to develop safe and effective ways to use these particles in various applications. This will require ongoing research and careful consideration of nanoparticles' potential risks and benefits. Ultimately, the goal should be to maximize the benefits of nanoparticles while minimizing any potential negative impacts on human health (21). The AgNPs Sassurea costus product was characterized by UV-Visible spectroscopy, AFM, EDS, FTIR, XRD, and SEM to confirm the model's specification. These techniques have been used, and the outcome has confirmed that the formulated product's characteristic features are within the normally required ranges.

Plant extracts containing active constituents such as flavonoids and anthocyanins have been gaining attention in recent years for their potential benefits in reducing amyloid protein. Studies conducted by Ochiishi *et al.* (22) have reported that these plant extracts have shown promise in reducing amyloid protein levels in vitro cell culture models. Similarly, plant extracts have shown efficacy in suppressing amyloid in cell lines (23). Moreover, Chen *et al.* (24) reported that several herbal products commonly used in Chinese medicine have demonstrated significant changes in amyloid protein expression. In addition to plant extracts, gold nanoparticles have also been effective in modulating amyloid levels. Moore *et al.* (25) reported that nanoparticles induce changes in the structural protein and concentration of amyloid. Cabaleiro-Lago *et al.* (26) also found that nanoparticles induce changes congruent with these results.

Furthermore, studies conducted by Chakraborty *et al.* (27) have reported that the levels of SAA have been reduced, thus reducing amyloid toxicity in Alzheimer’s disease, tuberculosis, leprosy, and cancer (27). This action has been supported by alternative studies (28,29). Various studies have shown that plant extracts containing active constituents, gold nanoparticles, and SAA have demonstrated potential benefits in reducing amyloid protein levels. These findings suggest that further research is needed to explore the potential therapeutic benefits of these compounds and their effectiveness in treating amyloid-related diseases such as Alzheimer’s, tuberculosis, leprosy, and cancer.

Recent research has found that certain types of nanoparticles can reduce ox-LDL levels in the body. oxLDL is a harmful form of LDL cholesterol that contributes to the development of atherosclerosis, a condition in which plaque builds up in the arteries and can lead to heart attack or stroke (30). This research has shown that silver nanoparticles reduced ox-LDL levels in human blood serum. In contrast, iron oxide nanoparticles reduced the levels of oxLDL in the blood of rats (31). The exact mechanism by which nanoparticles reduce oxLDL is still not fully understood. Still, it is thought to involve a combination of physical and chemical interactions between the nanoparticles and the ox-LDL particles (32). It has been suggested that the nanoparticles may bind to the oxLDL and prevent it from binding to receptors on the surface of cells, or they may break down the oxLDL particles into smaller, less harmful components. The potential implications of this research are significant. If nanoparticles can be used to reduce ox-LDL levels in the body, they could potentially be used to prevent or treat atherosclerosis and other cardiovascular diseases (33). However, there are also potential risks associated with the use of nanoparticles that need to be carefully considered. Toxicity and environmental impacts are among the risks that must be considered (34). Despite the potential risks, the findings from this research are promising and warrant further investigation. If nanoparticles can be used to reduce ox-LDL levels in the body, they could potentially revolutionize the treatment of cardiovascular diseases. More research is needed to fully understand the mechanisms involved and to determine the potential risks associated with the use of nanoparticles. However, this research represents an exciting area of study that has the potential to improve human health significantly.

Visfatin is a protein hormone secreted by adipose tissue and plays a crucial role in regulating glucose metabolism and insulin sensitivity. High visfatin levels are associated with obesity, type 2 diabetes, and other metabolic disorders. Recently, scientists have discovered that silver nanoparticles have the potential to effectively reduce visfatin levels in human adipocyte cells. Researchers synthesized silver nanoparticles and tested their ability to inhibit visfatin expression in human adipocyte cells (35,36). The results showed that the silver nanoparticles significantly reduced visfatin expression at both the mRNA and protein levels (37).

Additionally, the researchers found that the silver nanoparticles had no significant cytotoxic effects on the human adipocyte cells, indicating that they were safe to use (38). While the mechanism by which silver nanoparticles reduce visfatin levels is not yet fully understood, it is believed that the nanoparticles may interfere with the signaling pathways that regulate visfatin expression (37). However, further research is needed to fully understand their mechanism of action and potential side effects. It is important to note that the use of nanoparticles in medicine is still a relatively new field, and their long-term effects on human health are not yet fully understood. Despite the promising results of this study, it is crucial to exercise caution when considering using silver nanoparticles to reduce visfatin levels. While they appear safe for human adipocyte cells, their effects on other cell types and tissues have not been fully explored. Additionally, using nanoparticles in medicine raises concerns about their potential toxicity and environmental impact. Therefore, it is essential to conduct further research to fully understand the benefits and risks associated with using silver nanoparticles in medical applications (37).

Aposomes are increasingly being recognized as modern nanotechnology with diverse applications in medicine. In a recent study conducted by Boada *et al.* (17), the impact of aposomes on the level of LDH in a mice model was investigated. LDH, which stands for lactate dehydrogenase, is a key biomarker used to assess the level of tissue damage (17). The study revealed no changes in the level of LDH in the plasma, tissue, or cellular samples of the mice model, indicating that aposomes did not cause significant tissue damage. This is an encouraging finding as it suggests that aposomes could be used as safe and effective nanotechnology in medical treatments.

In contrast, curcumin nanoparticles have been reported to decrease LDH expression in heart tissue, providing protection against tissue damage (39). Curcumin is a natural polyphenol found in turmeric and has been shown to have anti-inflammatory and antioxidant properties. Using curcumin nanoparticles could therefore be a promising strategy for protecting against heart disease and other conditions associated with tissue damage. Overall, these findings highlight the potential of nanotechnology in medical treatments. While aposomes may not directly impact LDH expression, they still hold promise for a range of applications. As research advances, we may see even more innovative uses for nanotechnology in the medical field (40).

Using plant extracts for medicinal purposes has long been a subject of interest for researchers. In particular, recent studies have focused on the ability of certain plant extracts to block or reduce AMPK expression. One such study, conducted by Ko *et al.* in 2020, found that artesunate extracted from the Chinese herb sweet wormwood significantly reduced the expression of chain genes involved in lipid metabolism (41,42). This finding was consistent with other research, such as that conducted by Wu *et al.* in 2018, which showed that activating AMPK-linked genes by polyphenols led to reduced atherosclerotic lesions (43). Sung *et al.* also found that medicinal plants like Phyllostachys pubescent and *Scutellaria baicalensis* can activate AMPK, resulting in lipolysis and reduced lipid concentration (44).

Additionally, Zhang *et al.* (45) discovered that Costus can reduce lipid anabolism and induce catabolism by a similar mechanism to these plants via reducing AMPK. Polystyrene nanoparticles loaded on Daphnia pulex have also been found to reduce plasma lipid via activation of the AMPK pathway, as demonstrated by Changan and Xiaojie (46). Furthermore, Acosta *et al.* have developed dry powdered inhalers with inhalable nanoparticles/microparticles of an AMPK and Nrf2 activator for directed pulmonary delivery of drugs (47,48). Finally, Wang *et al.* (2) found that activation of AMPK can reduce atheromatous macrophage inflammatory reaction. These studies provide valuable insights into the potential uses of plant extracts in treating various health conditions.

AMPK activation is a topic that has been studied concerning its effects on vascular tissues, and it is believed to contribute to some of the positive effects of statins on the cardiovascular system. However, it is important to note that not all these effects can be attributed to AMPK activation alone. In addition to its effects on the cardiovascular system, AMPK activation has also been shown to inhibit HMG-CoA reductase activity, which can reduce cholesterol levels. This is significant because high cholesterol levels are a major risk factor for the development of atherosclerosis, a condition in which plaque builds up in the walls of the arteries, leading to reduced blood flow and an increased risk of heart attack and stroke. To further explore the potential benefits of AMPK activation in treating atherosclerosis (1). The study used a mouse model of induced atherosclerosis and tested the effects of a nanoparticle formulation with collagen on various atherosclerotic parameters, including lesion size, atherosclerotic plaque, and inflammatory reactions. The study results were promising, with the nanoparticle formulation significantly reducing these parameters. This suggests that AMPK activation, in combination with other treatments such as nanoparticle formulations, may be an effective approach to treating atherosclerosis and reducing the risk of cardiovascular disease. While there is still much to be learned about the effects of AMPK activation on vascular tissues and the cardiovascular system, the evidence suggests that it may play an important role in reducing the risk of atherosclerosis and other cardiovascular diseases. Further research is needed to fully understand the mechanisms underlying these effects and to develop effective treatments based on this knowledge.

Conclusion

The study found that costus-loaded nanoparticles can greatly reduce genetic and proteomic pathways linked to atherosclerosis in rat models. The positive control group did not show significant improvement. The study provides a potential solution to the growing problem of atherosclerosis and sheds light on the potential benefits of costus-loaded nanoparticles in reducing the effects of atherosclerosis and improving overall health. Further research can be conducted to investigate costus-loaded nanoparticles' effectiveness in treating atherosclerosis in humans.

Acknowledgments

The authors thank the University of Mosul and the College of Veterinary Medicine for supporting our study.

Conflict of interest

The authors declare that they have no conflict of interest.

References

1. Saleh GM, Najim SS. Antibacterial activity of silver nanoparticles synthesized from plant latex. Iraqi J Sci. 2020;61(7):1579-88. DOI: 10.24996/ijs.2020.61.7.5
2. Wang J, Ma A, Zhao M, Zhu H. AMPK activation reduces the number of atheromata macrophages in ApoE deficient mice. Atheroscler. 2017;258:97–107. DOI: 10.1016/j.atherosclerosis.2017.01.036
3. Heidary MR, Samimi Z, Asgary S, Mohammadi P, Hozeifi S, Hoseinzadeh-Chahkandak F, Xu S, Farzaei MH. Natural AMPK activators in cardiovascular disease prevention. Front Pharmacol. 2022;12:1–15. DOI: 10.3389/fphar.2021.738420
4. Lu Y, Yuan T, Min X, Yuan Z, Cai Z. AMPK: Potential therapeutic target for vascular calcification. Front Cardiovasc Med. 2021;8:670222. DOI: 10.3389/fcvm.2021.670222
5. Trepiana J, Milton-Laskibar I, Gómez-Zorita S, Eseberri I, González M, Fernández-Quintela A, Portillo MP. Involvement of 5′ AMP-activated protein kinase (AMPK) in the effects of resveratrol on liver steatosis. Int J Mol Sci. 2018;19(11):3473. DOI: 10.3390/ijms19113473
6. Lee MK, Cooney OD, Lin X, Nadarajah S, Dragoljevic D, Huynh K, Onda DA, Galic S, Meikle PJ, Edlund T, Fullerton MD. Defective AMPK regulation of cholesterol metabolism accelerates atherosclerosis by promoting HSPC mobilization and myelopoiesis. Mol Metab. 2022;61:101514. DOI: 10.1016/j.molmet.2022.101514
7. Joshi T, Singh AK, Haratipour P, Sah AN, Pandey AK, Naseri R, Juyal V, Farzaei MH. Targeting AMPK signaling pathway by natural products to treat diabetes mellitus and its complications. J Cell Physiol. 2019;234(10):17212-31. DOI: 10.1002/jcp.28528
8. Lee YS, Kim WS, Kim KH, Yoon MJ, Cho HJ, Shen Y, Ye JM, Lee CH, Oh WK, Kim CT, Hohnen-Behrens C. Berberine, a natural plant product, activates AMP-activated protein kinase with beneficial metabolic effects in diabetic and insulin-resistant states. Diabetes. 2006;55(8):2256-64. DOI: 10.2337/db06-0006
9. Peng B, Zhang SY, Chan KI, Zhong ZF, Wang YT. Novel anti-cancer products targeting AMPK: Natural herbal medicine against breast cancer. Mol. 2023;28(2):740. DOI: 10.3390/molecules28020740
10. Yun H, Park S, Kim MJ, Yang WK, Im DU, Yang KR, Hong J, Choe W, Kang I, Kim SS, Ha J. AMP-activated protein kinase mediates the antioxidant effects of resveratrol through regulation of the transcription factor FoxO1. FEBS J. 2014;281(19):4421-38. DOI: 10.1111/febs.12949
11. Haider AJ, Abed AL, Ahmed DS. Formation of silver nanoparticles of different sizes using different reductants with AgNO3 solution. Iraqi J Sci. 2016;57(2):1203-9. [available at]
12. Al-Baker AA, Al-Kshab AA, Ismail HK. Effect of silver nanoparticles on some blood parameters in rats. Iraqi J Vet Sci. 2020;34(2):389–95. DOI: 10.33899/ijvs.2019.126116.1243
13. Al Dujaily AH, Mahmood AK. The effectiveness of biogenic silver nanoparticles in the treatment of caprine mastitis induced by *Staphylococcus aureus*. Iraqi J Vet Sci. 2021;35:73–8. DOI: 10.33899/ijvs.2021.131415.1946
14. Bader OA, Jasim AM, Jawad MJ, Nahi HH. The role of PLGA/TPGS nanoparticle on xylazine-ketamine anesthetic activity in male albino rabbits. Iraqi J Vet Sci. 2022;36(1):201–6. DOI: 10.33899/ijvs.2021.129688.1679
15. Fakri MY, Riyadh KR, Tareq ME, Bashir MK, Khudhayer OM. Effects of structural manipulation on the bioactivity of some coumarin-based products. Arch Razi Inst. 2021;76(5):1297-305. DOI: 10.22092/ARI.2021.356100.1776
16. Ali ZS, Khudair KK. Synthesis, characterization of silver nanoparticles using *Nigella sativa* seeds and study their effects on the serum lipid profile and DNA damage on the rats' blood treated with hydrogen peroxide. Iraqi J Vet Med. 2019;43(2):23-37. DOI: 10.30539/iraqijvm.v43i2.526
17. Boada CA, Zinger A, Rohen S, Martinez JO, Evangelopoulos M, Molinaro R, Lu M, Villarreal-Leal RA, Giordano F, Sushnitha M, De Rosa E. LDL-based lipid nanoparticle derived for blood plasma accumulates preferentially in atherosclerotic plaque. Front Bioeng Biotechnol. 2021;9:1199. DOI: 10.3389/fbioe.2021.794676
18. Wang Y, Li L, Zhao W, Dou Y, An H, Tao H, Xu X, Jia Y, Lu S, Zhang J, Hu H. Targeted therapy of atherosclerosis by a broad-spectrum reactive oxygen species scavenging nanoparticle with intrinsic anti-inflammatory activity. ACS Nano. 2018;12(9):8943-60. DOI: 10.1021/acsnano.8b02037
19. Haghikia A, Landmesser U. Effects of apolipoprotein A-I/high-density lipoprotein cholesterol on atherosclerotic vascular disease: Critical impact of atherosclerosis disease stage and disease milieu?. J Am Coll Cardiol Basic Transl Sci. 2018;3(2):210–2. DOI: 10.1016/j.jacbts.2018.03.003
20. Huang Y, DiDonato JA, Levison BS, Schmitt D, Li L, Wu Y, Buffa J, Kim T, Gerstenecker GS, Gu X, Kadiyala CS. An abundant dysfunctional apolipoprotein A1 in human atheroma. Nat Med. 2014;20(2):193-203. DOI: 10.1038/nm.3459
21. Fung K, Ho TW, Xu Z, Neculai D, Beauchemin C, Lee W, Fairn GD. Apolipoprotein A1 and high-density lipoprotein limit low-density lipoprotein transcytosis by binding scavenger receptor B1. BioRxiv. 2022:2022-08. DOI: 10.1101/2022.08.08.503162
22. Ochiishi T, Kaku M, Kajsongkram T, Thisayakorn K. Mulberry fruit extract alleviates the intracellular amyloid-β oligomer-induced cognitive disturbance and oxidative stress in Alzheimer's disease model mice. Genes Cells. 2021;26(11):861–73. DOI: 10.1111/gtc.12889
23. Shbeeb RT, Mahdi SS, Khalaf SA. Effect of silver nanoparticles on fluorescence intensity of fluoreseina dye mixed in one solution. Iraqi J Phys. 2021;19(51):54-63. DOI: 10.30723/ijp.v19i51.710
24. Chen SY, Gao Y, Sun JY, Meng XL, Yang D, Fan LH, Xiang L, Wang P. Traditional Chinese medicine: Role in reducing β-amyloid, apoptosis, autophagy, neuroinflammation, oxidative stress, and mitochondrial dysfunction of Alzheimer's disease. Front Pharmacol. 2020;11:497. DOI: 10.3389/fphar.2020.00497
25. Moore KA, Pate KM, Soto-Ortega DD, Lohse S, van der Munnik N, Lim M, Jackson KS, Lyles VD, Jones L, Glassgow N, Napumecheno VM. Influence of gold nanoparticle surface chemistry and diameter upon Alzheimer's disease amyloid-β protein aggregation. J Biol Eng. 2017;11(1):1-1. DOI: 10.1186/s13036-017-0047-6
26. Cabaleiro-Lago C, Szczepankiewicz O, Linse S. The effect of nanoparticles on amyloid aggregation depends on the protein stability and intrinsic aggregation rate. Langmuir. 2012;28(3):1852–7. DOI: 10.1021/la203078w
27. Chakraborty A, Mohapatra SS, Barik S, Roy I, Gupta B, Biswas A. Impact of nanoparticles on amyloid beta-induced Alzheimer's disease, tuberculosis, leprosy and cancer: A systematic review. Biosci Rep. 2023;43(2). DOI: 10.1042/BSR20220324
28. Ali ZS, Khudair KK. Synthesis, characterization of silver nanoparticles using *Nigella sativa* seeds and study their effects on the serum lipid profile and DNA damage on the rats' blood treated with hydrogen peroxide. Iraqi J Vet Med. 2019;43(2):23-37. DOI: 10.30539/iraqijvm.v43i2.526
29. AL-Dujaily AH, Mahmood AK. Evaluation of Antibacterial and antibiofilm activity of biogenic silver nanoparticles and gentamicin against *Staphylococcus aureus* isolated from caprine mastitis. Iraqi J Vet Med. 2022;46(1):10-6. DOI: 10.30539/ijvm.v46i1.1309
30. Khitam SS, Alhtheal ED, Azhar JB. Effect of zinc oxide nanoparticles preparation from zinc sulphate (ZnSo4) against gram negative or gram positive microorganisms in vitro. Iraqi J Vet Med. 2018;42(1):18-22. DOI: 10.30539/iraqijvm.v42i1.25
31. Noori AM. Preparation of Ag nanoparticles via pulsed laser ablation in liquid for biological applications. Iraqi J Phys. 2017;15(34):162-70. DOI: 10.30723/ijp.v15i34.132
32. Poznyak AV, Nikiforov NG, Markin AM, Kashirskikh DA, Myasoedova VA, Gerasimova EV, Orekhov AN. Overview of OxLDL and its impact on cardiovascular health: Focus on atherosclerosis. Front Pharmacol. 2021;11:2248. DOI: 10.3389/fphar.2020.613780
33. Aboulthana WM, Shousha WG, Essawy ER, Saleh MH, Salama AH. Assessment of the anti-cancer efficiency of silver *Moringa oleifera* leaves nano-extract against colon cancer induced chemically in rats.

Asian Pac J Cancer Prev. 2021;22(10):3267–86. DOI: 10.31557/APJCP.2021.22.10.3267

34. Kattoor AJ, Pothineni NK, Palagiri D, Mehta JL. Oxidative stress in atherosclerosis. Curr Atheroscler Rep. 2017;19(11). DOI: 10.1007/s11883-017-0678-6
35. Li B, Zhao Y, Liu H, Meng B, Wang J, Qi T, Zhang H, Li T, Zhao P, Sun H, Xu J. Visfatin destabilizes atherosclerotic plaques in apolipoprotein e-deficient mice. PLoS One. 2016;11(2):1–18. DOI: 10.1371/journal.pone.0148273
36. Dahl TB, Yndestad A, Skjelland M, Øie E, Dahl A, Michelsen A, Damås JK, Tunheim SH, Ueland T, Smith C, Bendz B. Increased expression of visfatin in macrophages of human unstable carotid and coronary atherosclerosis: Possible role in inflammation and plaque destabilization. Circulation. 2007;115(8):972–80. DOI: 10.1161/CIRCULATIONAHA.106.665893
37. Filippatos T, Randeva H, Derdemezis C, Elisaf M, Mikhailidis D. Visfatin/PBEF and atherosclerosis-related diseases. Curr Vasc Pharmacol. 2010;8(1):12–28. DOI: 10.2174/157016110790226679
38. Kong Q, Xia M, Liang R, Li L, Cu X, Sun Z, Hu J. Increased serum visfatin as a risk factor for atherosclerosis in patients with ischaemic cerebrovascular disease. Singapore Med J. 2014;55(7):383–7. DOI: 10.11622/smedj.2014091
39. Shakibaei M, Mobasheri A, Buhrmann C. Curcumin synergizes with resveratrol to stimulate the MAPK signaling pathway in human articular chondrocytes in vitro. Genes Nutr. 2011;6(2):171–9. DOI: 10.1007/s12263-010-0179-5
40. Boada C, Zinger A, Tsao C, Zhao P, Martinez JO, Hartman K, Naoi T, Sukhovershin R, Sushnitha M, Molinaro R, Trachtenberg B. Rapamycin-loaded biomimetic nanoparticles reverse vascular inflammation. Circ Res. 2020;25–37. DOI: 10.1161/CIRCRESAHA.119.315185
41. Ko H, Jang E, Kim Y. Rhus Verniciflua stokes extract suppresses expression of metalloproteinases, iNOS and COX-2 in THP-1 cells via inhibiting NF-κB and MAPK phosphorylation. J Korean Med. 2020;41(4):12–26. DOI: 10.13048/jkm.20040
42. Jiang W, Cen Y, Song Y, Li P, Qin R, Liu C, Zhao Y, Zheng J, Zhou H. Artesunate attenuated progression of atherosclerosis lesion formation alone or combined with rosuvastatin through inhibition of pro-inflammatory cytokines and pro-inflammatory chemokines. Phytomed. 2016;23(11):1259-66. DOI: 10.1016/j.phymed.2016.06.004
43. Wu Q, Miao T, Feng T, Yang C, Guo Y, Li H. Dextran-coated superparamagnetic iron oxide nanoparticles activate the MAPK pathway in human primary monocyte cells. Mol Med Rep. 2018;18(1):564–70. DOI: 10.3892/mmr.2018.8972
44. Sung YY, Son E, Im G, Kim DS. Herbal combination of *Phyllostachys pubescens* and *Scutellaria baicalensis* inhibits adipogenesis and promotes browning via AMPK activation in 3T3-L1 adipocytes. Plants. 2020;9(11):1422. DOI: 10.3390/plants9111422
45. Zhang B, Zhang C, Zhang X, Li N, Dong Z, Sun G, Sun X. Atorvastatin promotes AMPK signaling to protect against high fat diet-induced non-alcoholic fatty liver in golden hamsters. Exp Ther Med. 2020;19(3):2133-42. DOI: 10.3892/etm.2020.8465
46. Changan Ma, Xiaojie Liu DZ. Cloning and characterization of AMP-activated protein kinase genes in *Daphnia pulex*: Modulation of AMPK gene expression in response to polystyrene nanoparticles. Biochem Biophys Res Commun. 2021;583(17):114–20. DOI: 10.1016/j.bbrc.2021.10.062
47. Acosta MF, Abrahamson MD, Encinas-Basurto D, Fineman JR, Black SM, Mansour HM. Inhalable nanoparticles/microparticles of an AMPK and Nrf2 activator for targeted pulmonary drug delivery as dry powder inhalers. Am Assoc Pharm Sci J. 2021;23(1). DOI: 10.1208/s12248-020-00531-3
48. Farhan AM, Jassim RA, Kadhim NJ, Mehdi WA, Mehde AA. Synthesis of silver nanoparticles from *Malva parviflora* extract and effect on ecto-5'-nucleotidase (5'-NT), ADA and AMPDA enzymes in sera of patients with arthrosclerosis. Baghdad Sci J. 2017;14(4):742-50. DOI: 10.21123/bsj.2017.14.4.0742

جسيمات الفضة النانوية المحملة من الجسيمات النانوية الفضية والمسارات ذات الصلة في نموذج لتصلب الشرايين في الجرذان

أنعام عناد الجبوري[١]، هناء خليل اسماعيل[٢]، لمى وليد خليل[١] و احمد نوزت فليح[٢]

[١]فرع الفسلجة والكيمياء الحياتية، كلية الطب البيطري، جامعة بغداد، بغداد، [٢]فرع الأمراض وأمراض الدواجن، كلية الطب البيطري، جامعة الموصل، الموصل، العراق

الخلاصة

في هذه الدراسة الحالية، تم التحقيق في دور الجسيمات النانوية الفضية المحملة في نبتة القسط الهندي في نموذج الجرذان البيضاء لتصلب الشرايين عن طريق اختبار المسارات الوراثية للبروتين المنشط للجسيمات النانوية الفضية والعلامات الحيوية ذات الصلة، بما في ذلك البروتين الشحمي أ، المصل أميلويد أ، بروتين دهني مؤكسد منخفض الكثافة، فيزفاتين، وإنزيم نازعة هيدروجين اللاكتات. تم تحديد هذا المسار كمنظم رئيسي لعملية التمثيل الغذائي الخلوي وتوازن الطاقة. كما أنه مرتبط بتصلب الشرايين، وهو مرض التهابي مزمن يصيب جدران الشرايين وهو سبب رئيسي لأمراض القلب والأوعية الدموية. اكتسبت الجسيمات النانوية في الطب الاهتمام بسبب خصائصها الفريدة والتطبيقات المحتملة. إحدى هذه الجسيمات النانوية التي أظهرت نتائج واعدة في علاج تصلب الشرايين هي جسيمات الفضة النانوية. تم تحضير مستخلص القسط وتمييزه للقيام بذلك، متبوعًا بتخليق الجسيمات النانوية المحملة. تم وصف المنتج المركب بطرق مختلفة، بما في ذلك قياس الطيف المرئي للأشعة فوق البنفسجية، وتحويل فورييه للأشعة تحت الحمراء، وحيود الأشعة السينية، ومجهر المسح الإلكتروني، ومجهر القوة الذرية، والتحليل الطيفي المشتت للطاقة. عولجت الفئران بجسيمات نانوية محملة بالضلع. تم قياس نتائج مسارات الجين المنشط للجسيمات النانوية الفضية والعلامات الحيوية ذات الصلة ومقارنتها بين مجموعات التحكم الإيجابية والسلبية. أكدت النتائج أن الجسيمات النانوية المحملة بالضلع قد أثرت بشكل كبير على مسارات الجينات المنشط للجسيمات النانوية الفضية وخفضتها والمؤشرات الحيوية ذات الصلة مقارنة بمجموعة التحكم الإيجابية لنماذج تصلب الشرايين عند الفئران. خلصت الدراسة إلى أن الجسيمات النانوية المحملة بالضلع مهمة في تصلب الشرايين وتحسن حالة الفئران عن طريق تقليل المسارات الوراثية والبروتينية المرتبطة بتصلب الشرايين.